

# Quantum Dynamics Study of Torsional Excitation of Glycine in Collision with Hydrogen Atom on *ab Initio* Potential Energy Surface<sup>†</sup>

Da W. Zhang, Ming L. Wang, and J. Z. H. Zhang\*

Department of Chemistry, New York University, New York, New York 10003

Received: January 10, 2003; In Final Form: February 19, 2003

Quantum mechanical study has been carried out to investigate C–C torsional excitation in glycine via collisional energy transfer with hydrogen atom. In this study, *ab initio* calculation is carried out to generate potential energies on a two-dimensional grid (torsional angle and radial coordinate) for given fixed orientational angle ( $\theta$ ,  $\phi$ ). These discrete energies are fitted with a local linear least-squares method to generate potential energies at any given point in two-dimensional space for dynamics calculation. Time-dependent quantum wave packet calculation is employed to study energy transfer to the C–C torsional mode of glycine, and state-to-state transition probabilities are obtained for different initial angles of collision. Strong angle-dependent energy transfer is observed from the calculation. Although the total energy transferred to the torsional mode is small, collision from certain angles can result in relatively large conformational change in torsion by as much as 30° degrees.

## I. Introduction

Understanding the mechanism of protein conformational change that controls folding and unfolding of protein is crucial to understanding the reactivity and mutation of proteins.<sup>1</sup> Because proteins are macromolecules consisting of a large number of atoms, theoretical study of protein dynamics is largely limited to classical mechanical treatment that solves Newton's equations of motion. Relatively few attempts have been made to employ quantum dynamical methods in protein dynamics studies.<sup>2</sup> Despite the huge success of classical simulations of proteins, there are still inherent limitations in classical treatment due to the classical nature of the approach. For example, quantum mechanical tunnelings that are associated with light hydrogen atoms could not be correctly described by classical mechanics. In addition, the zero point energies of the molecules are not preserved in classical simulation.<sup>3,4</sup> These problems are inherent in classical mechanics and their effects in biological molecules have not been fully investigated due to difficulties associated with quantum mechanical treatment of many body problems. Ideally, one would like to incorporate some or part of the quantum treatment in protein dynamics studies.

Because fundamental units of proteins are amino acids, a unique sequence of 20 amino acids completely determines a protein's structure (native structure) and therefore its particular biological function.<sup>5</sup> Because conformational change of a protein is largely caused by low-frequency torsional motions that control folding and unfolding of protein at normal temperatures,<sup>6</sup> studying torsional excitation in protein is of fundamental importance in protein dynamics. Furthermore, a protein performs its function through specific interactions of its amino acids with other atoms and molecules. Thus studying interaction dynamics of amino acids with individual atoms or molecules is of fundamental interest. Although a vast amount of molecular dynamics studies have been carried out to investigate energy transfer in protein interactions, theoretical works that study the detailed process of energy transfer for interaction with individual

amino acids are scarce. Because individual amino acids or small peptides are much smaller than proteins, it is possible to employ quantum mechanical methods to study interaction dynamics of amino acids with small atoms or molecules at accurate levels. It thus seems natural to explore the energy transfer process involving individual amino acids or small peptides to investigate their dynamical properties using quantum mechanical approaches.

In this paper, we present a quantum mechanical study of torsional inelastic scattering of glycine, the smallest amino acid, by a hydrogen atom. In our study, we treat the glycine as two rigid bodies connected by the C–C bond and solve the quantum scattering equation for collision of glycine with a hydrogen atom. Because glycine is the smallest amino acid with a small number of atoms, *ab initio* calculation of potential energy surface for hydrogen interaction with glycine is computationally feasible. To make quantum calculations efficient, however, approximation has been made to simplify the theoretical treatment. Because the main objective of the present study is to investigate C–C torsional excitation of glycine through collision with a hydrogen atom, we use a two-dimensional (2D) model to study quantum collision dynamics. Specifically, we fix the spatial orientational ( $\theta$ ,  $\phi$ ) of glycine in the dynamics calculation, which results in a 2D quantum scattering model: the radial coordinate  $R$  and torsional angle  $\chi$ . The 2D dynamics calculation is thus carried out for a fixed collision angle ( $\theta$ ,  $\phi$ ), which is varied in different dynamics calculations to investigate collision at different orientations. A recent theoretical study of energy transfer to glycine by collision with a hydrogen atom shows that energy transfer to overall rotational motion of glycine is quite small.<sup>7</sup> Thus the current 2D model with fixed orientation of glycine should be reasonable to study torsional excitation of glycine in collision with a hydrogen atom.

Because the current dynamics model is of low dimensionality, it is possible to study hydrogen–glycine collision dynamics *ab initio*. Thus in this study, we use density functional method (DFT) to calculate potential energies on a discrete two-dimensional grid of ( $R$ ,  $\chi$ ). The *ab initio* calculation is done for

<sup>†</sup> Part of the special issue "Donald J. Kouri Festschrift".

any given orientation ( $\theta$ ,  $\phi$ ). A local linear least-squares (LLS) fitting method<sup>16</sup> is then employed to generate potential energies at any given nuclear coordinates. The time-dependent quantum wave packet method is then employed to carry out inelastic collision calculation. State-to-state transition probabilities are computed, and results are discussed.

This paper is organized as follows: Section II gives a description of the theoretical treatment including the dynamical model, ab initio calculations, and the fitting of potential energy surface. Section III shows the results of the calculation with discussions, and section IV concludes.

## II. Theoretical Approach

**A. 2D Collision Model for Hydrogen–Glycine.** In our theoretical study of energy transfer to torsional motion of glycine by collision with a hydrogen atom, the glycine is treated as two rigid bodies connected by the C–C bond. The glycine is initially set at the “stretched” or *S* state, which is one of the two minimum conformations of glycine, with the other having the “cyclic” or *C* conformation.<sup>8</sup> The two conformers can interconvert from each other through rotation along the C–C bond with a barrier of 3.0 kcal/mol. Because we are mainly concerned with the C–C bond torsional motion, the C–C bond is fixed in space in the dynamics model. In addition, we also fix the attacking angles of the hydrogen atom. This is based on the assumption that the overall rotational motion of glycine is much slower than the translational motion, an approximation often termed infinite order sudden approximation (IOSA).<sup>9</sup> Thus for any fixed collision angle ( $\theta$ ,  $\phi$ ), we are dealing with a 2D quantum scattering problem that includes the radial coordinate of the hydrogen atom  $R$  and torsional angle  $\chi$  about the C–C bond.

The Hamiltonian for the 2D scattering problem is thus given by

$$\hat{H} = -\frac{\hbar^2}{2\mu} \frac{\partial^2}{\partial R^2} + \frac{L^2}{2\mu R^2} + \hat{H}_{\text{tor}}(\chi) + V(R, \chi; \theta, \phi) \quad (1)$$

where  $\mu$  is the reduced translational mass between the hydrogen atom and glycine,  $R$  is the radial distance from the hydrogen atom to the origin, which is fixed as the collision point on the C–C bond. In this study we treat the C–C bond as a fixed axis of rotation with two rigid groups attached at two ends. The one-dimensional Hamiltonian  $\hat{H}_{\text{tor}}(\chi)$  describing the torsional motion of glycine around the C–C bond is given by

$$\hat{H}_{\text{tor}} = -\frac{\hbar^2}{2I} \frac{\partial^2}{\partial \chi^2} + v(\chi) \quad (2)$$

where  $v(\chi)$  is the torsional potential,  $\chi$  is the torsional angle, and  $I$  is the reduced moment of inertia. We calculate the reduced moment of inertia for the torsional motion around the C–C bond as

$$I = \frac{I_{\text{COOH}} I_{\text{CH}_2\text{NH}_2}}{I_{\text{COOH}} + I_{\text{CH}_2\text{NH}_2}} \quad (3)$$

where  $I_{\text{COOH}}$  and  $I_{\text{CH}_2\text{NH}_2}$  are the moments of inertia along the C–C bond for the COOH group and CH<sub>2</sub>NH<sub>2</sub> group, respectively. As shown in Figure 1 for hydrogen–glycine scattering, the interaction potential  $V$  is a function of two internal coordinates ( $R$ ,  $\chi$ ), where  $R$  is the relative distance between the

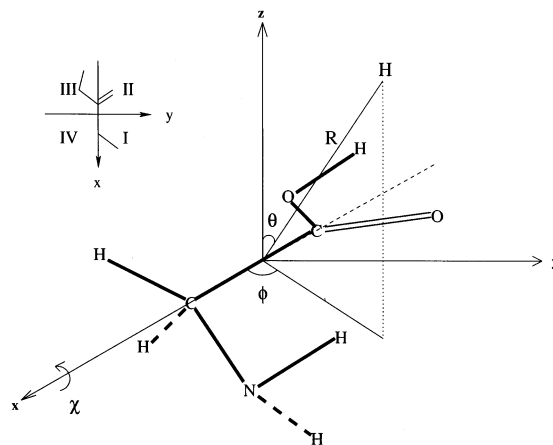


**Figure 1.** Geometry of glycine and the coordinates defined in the scattering model. The coordinate  $R$  is the distance from the hydrogen atom to the collision point on the C–C bond in glycine. The glycine is initially fixed at the *S* configuration.

hydrogen and the collision point on the C–C bond and  $\chi$  is the torsional angle of glycine along the C–C bond.

To solve the 2D scattering problem, we employ quantum wave packet approach<sup>10–12</sup> to solve the TD Schrödinger equation

$$i\hbar \frac{\partial}{\partial t} \Psi(t) = H\Psi(t) \quad (4)$$

with the Hamiltonian given by eq 1. With an appropriate choice of basis set, the TD wave function  $\Psi(t)$  is expanded as<sup>13</sup>

$$\Psi(t) = \sum_{nv} u_n(R) \phi_v(\chi) C_{nv}(t) \quad (5)$$

where particle-in-a-box plane wave function is used as the translational basis function  $u_n(R)$  and the torsional basis  $\phi_v(\chi)$  is given by solving the one-dimensional eigenfunction

$$\left[ -\frac{\hbar^2}{2I} \frac{\partial^2}{\partial \chi^2} + v(\chi) \right] \phi_v(\chi) = \epsilon_v \phi_v(\chi) \quad (6)$$

The one-dimensional Schrödinger equation for torsional angle with this Hamiltonian given by eq 2 can be solved by the standard basis set method using sine and cosine basis functions.

The TD wave function is propagated using the split-operator method<sup>14</sup>

$$\Psi(t + \Delta) = e^{-i\hat{H}_0\Delta/2} e^{-i\hat{U}\Delta} e^{-i\hat{H}_0\Delta/2} \Psi(t) \quad (7)$$

The operator  $\hat{H}_0$  is chosen to be

$$\hat{H}_0 = -\frac{\hbar^2}{2\mu} \frac{\partial^2}{\partial R^2} + \hat{H}_{\text{tor}} \quad (8)$$

where  $\hat{H}_{\text{tor}}$  is the torsional Hamiltonian given in eq 2. The generalized potential operator  $\hat{U}$  is given by

$$\hat{U} = \frac{L^2}{2\mu R^2} + \hat{V}(R, \chi; \theta, \phi) \quad (9)$$

In the present study, the orbital angular momentum  $L$  is chosen to be zero, which corresponds to s-wave scattering.

Because the dynamics scattering calculation is carried out for various collision angles, one could average over orientations

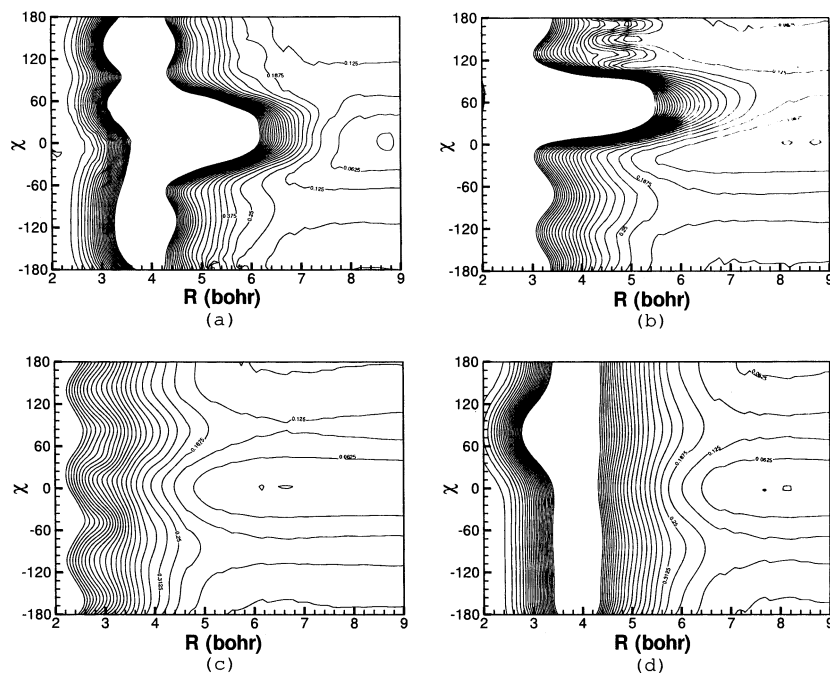


**Figure 2.** Contour plots of potential energy surface as a function of  $(R, \chi)$  at fixed collision angles  $(\theta, \phi)$ : (a)  $(80^\circ, 40^\circ)$ ; (b)  $(40^\circ, 60^\circ)$ ; (c)  $(20^\circ, 120^\circ)$ ; (d)  $(60^\circ, 240^\circ)$ .

**TABLE 1: Grids Used in LLLS Fitting of H+Glycine PES**

coordinate	no. of points	original grid set														
$R (a_0)$	15	2.0	2.5	3.0	3.5	4.0	4.5	5.0	5.5	6.0	6.5	7.0	7.5	8.0	8.5	9.0
$\chi$ (deg)	18	$-180 + n \times 20$ ( $n=0, \dots, 17$ )														

to obtain averaged physical quantity such as transition probability and the ratio of energy transfer. Using  $F$  to represent any of the desired physical quantities, its angle-averaged value can be obtained by simple integration over initial collision angles

$$\bar{F} = \frac{1}{4\pi} \int_0^\pi \int_0^{2\pi} F(\theta, \phi) \sin \theta \, d\theta \, d\phi \quad (10)$$

**B. Ab Initio Potential Energy Surface.** Because we are not aware of any available ab initio potential energy surface for the current hydrogen–glycine scattering, we need to construct a two-dimensional potential surface for dynamics calculation for any given set of collision angle  $(\theta, \phi)$ . Because glycine is planar, we place it in the  $XY$  plane of the Cartesian coordinate system and make the C–C bond coincide with the  $X$  axis, as shown in Figure 1. For any fixed orientation  $(\theta, \phi)$ , the potential surface depends on two internal coordinates  $(R, \chi)$ , as shown in Figure 1. DFT (density functional theory) calculation is thus carried out to generate discrete potential energies in this two-dimensional space on a  $15 \times 18$  grid for a given fixed orientation  $(\theta, \phi)$ . Utilizing the  $C_s$  symmetry of glycine, we only need to consider collisions with the polar angle  $\theta$  in the range  $[0, 90^\circ]$ . Table 1 lists the two-dimensional grid for which DFT calculation is performed to generate energies for a given collision angle. This is done for  $\theta$  in the range of  $[0, 90^\circ]$  and  $\phi$  in the range of  $[0, 360^\circ]$  with a constant spacing of  $20^\circ$ .

After ab initio points are generated by DFT calculation, the potential surface is fitted to give potential energy values at any desired point in space. In previous studies, we proposed a local least-squares fitting (LLLS) approach for numerical fitting of the potential surface from an arbitrary set of ab initio data.<sup>7,16</sup> In the LLLS approach, we expand the unknown potential  $V$  in

a basis set<sup>16</sup>

$$V = \sum_i c_i u_i \quad (11)$$

where  $c_i$  are the expansion coefficients to be determined. An energy cutoff criterion is used to eliminate points whose energies are above a certain cutoff limit. In our approach, the basis functions  $u_i$  are chosen to be localized Gaussian functions, one for each energy point. With local fitting strategy, only part of the energy points within a given range of the multidimensional space is included in the least-squares fitting. More details of this local least-squares fitting strategy can be found elsewhere.<sup>16</sup>

Figure 2 shows contour plots of the fitted potential energy surface as function of the radial coordinate  $R$  and torsional angle  $\chi$  at fixed collision angles of  $(80^\circ, 40^\circ)$ ,  $(40^\circ, 60^\circ)$ ,  $(20^\circ, 120^\circ)$ , and  $(60^\circ, 240^\circ)$ , respectively. As can be seen from the figure, these potentials are strongly dependent on the collision angle and result in angle-dependent energy transfer to the torsion.

### III. Results of Numerical Calculation

Geometry optimization of glycine is performed by DFT/B3LYP with a 6-31G(d) basis set using Gaussian98<sup>15</sup> to find the global minimum. The lowest minimum corresponds to the S (or stretched) configuration. Another stable configuration is the C (or cyclic) configuration, which differs from the S configuration through a  $180^\circ$  torsional rotation around the C–C bond defined in Figure 1. As shown in Figure 3, this C configuration is about 1.1 kcal/mol in energy above the S configuration. This result is consistent with other ab initio calculations in which the lowest C configuration was found to be higher in energy than that of the S configuration.<sup>8</sup> Although

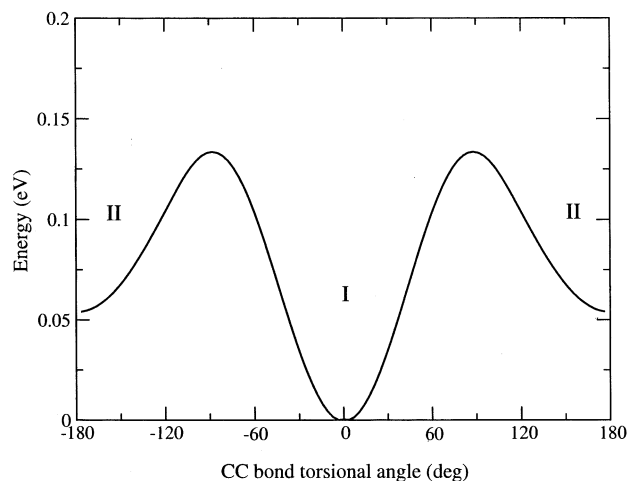


Figure 3. Torsional potential as a function of torsional angle in glycine.

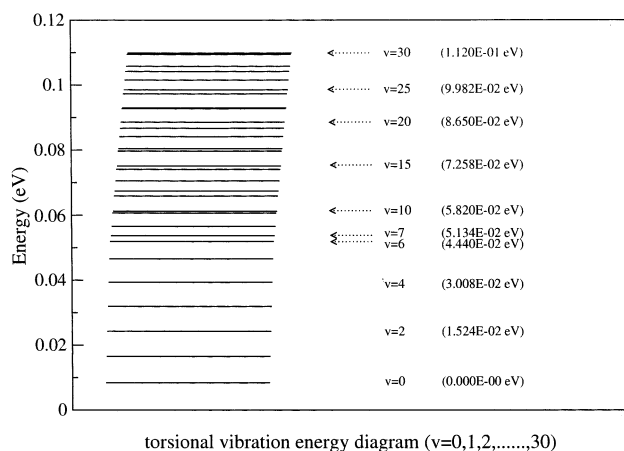


Figure 4. Torsional energy levels of glycine.

the C configuration in Figure 3 is not the absolute minimum of the C structure due to constraints of other degrees of freedom, the difference in energy from its absolute minimum is small. Therefore no significant effect is expected in the dynamics calculation due to this small structural deviation of the C configuration.

Using the global potential energy surface generated from the previous section, we carry out TD wave packet calculation to study torsionally inelastic scattering of glycine by hydrogen atom. A total of 60 particle-in-a-box sine functions are used to expand the radial dependence of the wave function spanning a distance of 2.0–14.5 bohr. For torsional motion, 30 vibrational functions are used in the expansion for the  $\chi$  dependence of the wave function. The initial wave packet  $\varphi_{k0}(R)$  is chosen to be a standard Gaussian function

$$\varphi_{k0}(R) = \left(\frac{1}{\pi\delta^2}\right)^{1/4} \exp[-(R - R_0)^2/2\delta^2] e^{-i\sqrt{2\mu E_0}R} \quad (12)$$

with Gaussian width  $\delta = 0.45$  and initial kinetic energy  $E_0 = 0.40$  eV. Figure 3 shows torsional potential curve of glycine. The periodic potential has a double-well shape with about 0.05 eV difference in depth. The two wells corresponds to the S and C structure of glycine, with a potential barrier of about 0.135 eV from the S to the C structure. Figure 4 shows the calculated torsional eigenvalues of the glycine. Among these eigenstates, the ground state belongs to the S configuration whereas the  $v = 7$  state is the lowest energy state in C configuration. Above  $v = 7$ , the wave functions become delocalized due to tunneling and exhibit double-well structure, as shown in Figure 4.

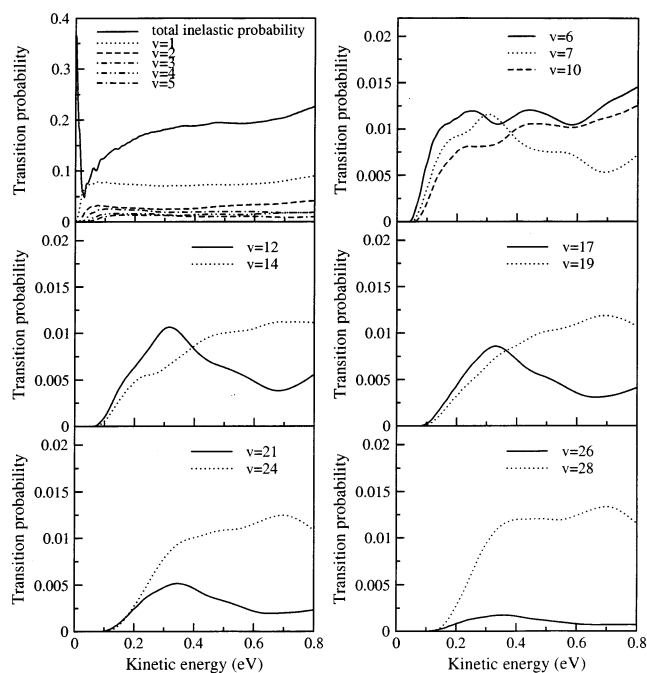


Figure 5. Angle-averaged inelastic transition probabilities from the ground state to excited torsional states as a function of collision energy.

Scattering calculations are carried out for various fixed values of collision angle ( $\theta$ ,  $\phi$ ), with glycine at ground state initially. Figure 5 shows the calculated state-to-state inelastic transition probabilities for torsional excitation to  $v = 1$  to  $v = 30$  as functions of kinetic energy. These probabilities are obtained by averaging the corresponding angle-dependent transition probabilities over all collision angles. As seen from the figure, the individual state-specific transition probability is generally small, with the largest transition going to the first excited state ( $v = 1$ ). Most individual probabilities are on the order of 1%. As the excitation increases, the threshold energy gradually increases as well. The total inelastic transition is fairly significant, about 20 as shown in Figure 5.

We next examine T–T (translational to torsional) energy transfer. This can be measured by the percentage of initial collision energy that is converted to the torsional energy of glycine, defined as

$$E_{\text{eff}} = \frac{E_f - E_0}{E_{\text{coll}}} \quad (13)$$

where  $E_f$  is the torsional excitation energy calculated by

$$E_f = \sum_v \epsilon_v P_v \quad (14)$$

where  $E_0$  is the initial (ground-state) energy of glycine,  $E_{\text{coll}}$  is the collision energy,  $\epsilon_v$  is the excited torsional eigen energy, and  $P_v$  is the corresponding excitation probability.

Figure 6 shows the value of  $E_{\text{eff}}$  as a function of collision energy for collision at various spherical angles of collision. There is a strong dependence on collision angles for energy transfer. For hydrogen approaching glycine perpendicular to the plane ( $\theta = 0^\circ$ ), the energy transfer to the torsional motion is very small, about 1.5%, as shown in Figure 6. For hydrogen approaching near parallel to the plane ( $\theta = 80^\circ$ ), energy transfer is also small, average about 2–3%. The largest energy transfer occurs for collision near  $\theta = 40^\circ$ , with an efficiency as high as 40% for certain azimuthal angle  $\phi$ . As shown in Figure 6, the

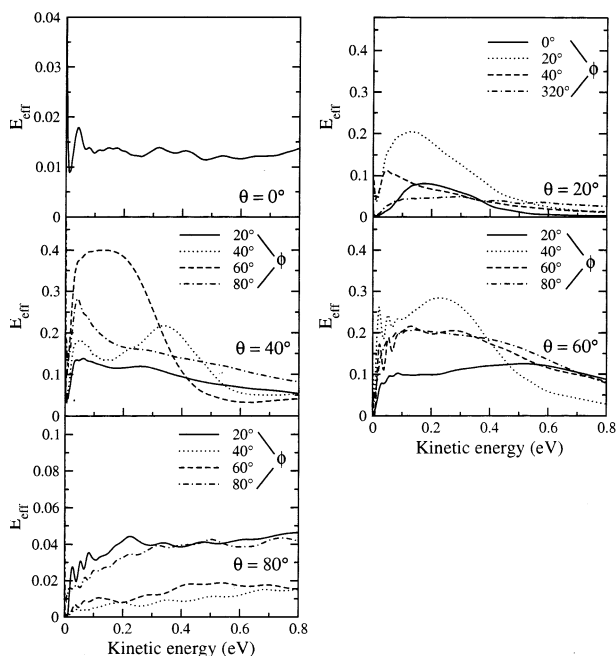


**Figure 6.** Individual T–T (translational  $\rightarrow$  torsional) energy transfer efficiency at different collision angle ( $\theta$ ,  $\phi$ ) as a function of collision energy.

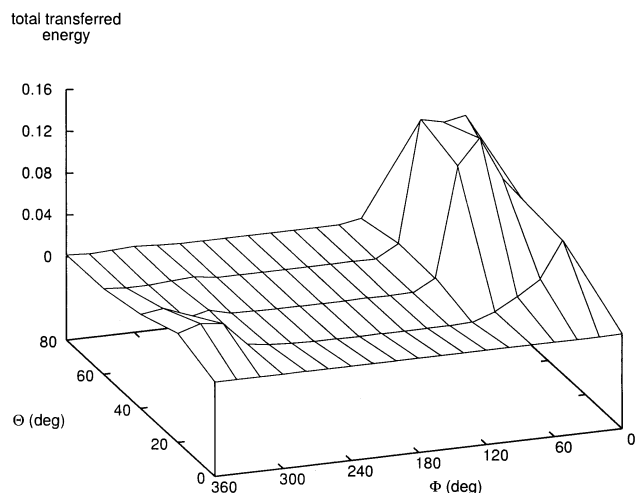


**Figure 7.** 3D plot of energy transfer as a function of collision angle ( $\theta$ ,  $\phi$ ).

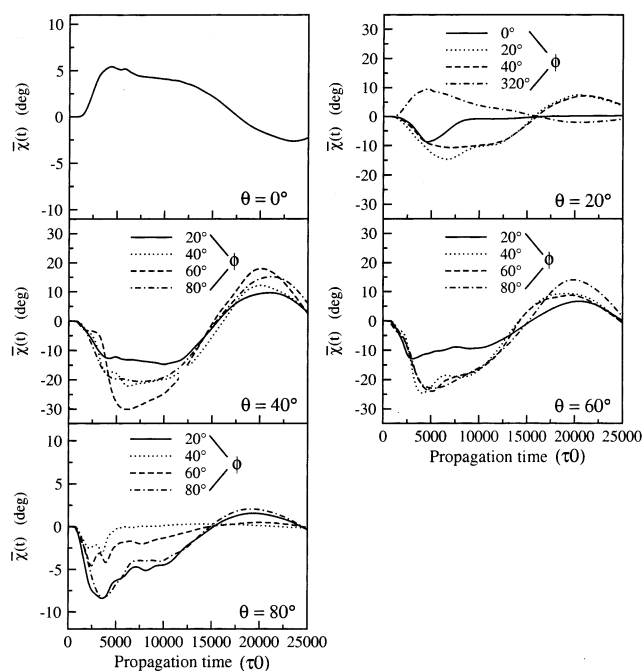
energy transfer efficiency is also dependent on the azimuthal angle. In general, the efficiency of energy transfer (percentage) is larger at small collision energy.

Figure 7 shows a 3D plot of  $E_{\text{eff}}$  over collision angles ( $\theta$ ,  $\phi$ ), in which relatively large energy transfer occurs within a small range of solid angles where the hydrogen atom approaches the glycine from region I (shown in bird's-eye view in Figure 1). For hydrogen attacking from regions II and III, in which the hydrogen approaches the C–C bond from the C terminal, the energy transfer to torsion is negligible.

Next, we examine the time dependence of the average value of torsional angle defined as

$$\bar{\chi}(t) = \langle \Psi(R, \chi, t) | \chi | \Psi(R, \chi, t) \rangle \quad (15)$$

where  $\chi$  is the torsional angle and  $\Psi(R, \chi, t)$  is the TD wave function at any given time  $t$ . Figure 8 shows the calculated average value of torsional angle as a function of time for various collision angles. Because glycine is initially at the ground state,



**Figure 8.** Mean torsional angle as a function of time for different collision angles ( $\theta$ ,  $\phi$ ). The initial Gaussian wave packet has a width  $\delta = 0.45$  and initial kinetic energy  $E_0 = 0.40$  eV.

the initial value of  $\bar{\chi}(t)$  is zero, as shown in the figure. Consistent with energy transfer shown in Figure 6, the high excitation of the torsional angle occurs near  $\theta = 40^\circ$ . The oscillatory structure shown in the figure simply represents that the excited torsional wave function is exercising quasi-periodic motion near the bottom of the potential well in Figure 3, after the collision event is completed.

To see the fluctuation of torsional angle away from the average value as a result of collision, we calculate the variance of the torsional angle as a function of collisional time by

$$\Delta\chi(t) = \sqrt{\langle \Psi(R, \chi, t) | (\chi - \bar{\chi})^2 | \Psi(R, \chi, t) \rangle} \quad (16)$$

Figure 9 shows  $\Delta\chi(t)$  for various collision angles as a function of propagation time. Similar to Figure 8, large variance is observed at those angles at which the energy transfer to torsion is enhanced. Like  $\bar{\chi}(t)$  in Figure 8,  $\Delta\chi(t)$  also oscillates in time after collision with hydrogen.

#### IV. Conclusion

A two-dimensional torsionally inelastic scattering model for hydrogen–glycine is presented in which the glycine is treated as two rigid bodies connected by the C–C bond. For a given collision angle ( $\theta$ ,  $\phi$ ), the two-dimensional potential energy surface is constructed from DFT quantum chemistry calculations that are fitted into a surface using the LLLS approach. Time-dependent quantum scattering calculations are carried out to obtain state-to-state transition probabilities. The energy transfer to the torsional mode is examined for various collision angles ( $\theta$ ,  $\phi$ ) of hydrogen. The results of the current study can be summarized as follows:

1. The individual state-to-state transition probability is generally small and the total inelastic transition probability is around 20%.

2. The efficiency of T–T energy transfer is strongly dependent on the initial collision angle. Although collisions from most orientational angles result in small energy transfer, attacking

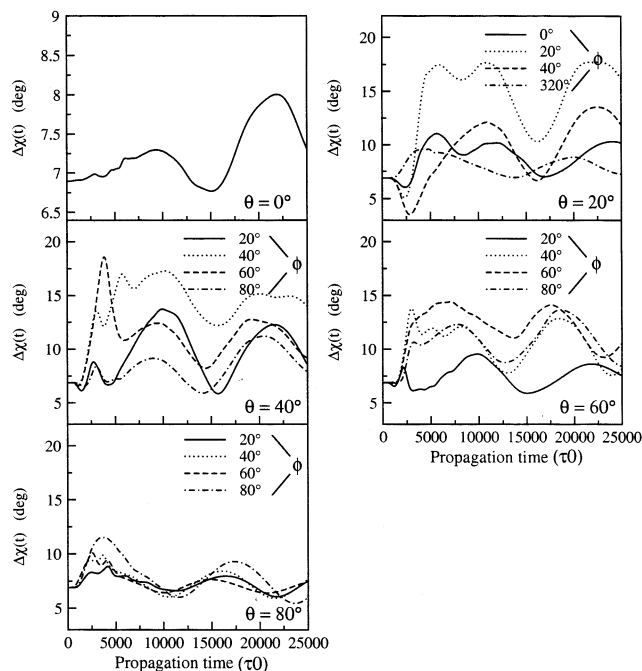


**Figure 9.** Variance of the torsional angle as a function of time at different collision angles ( $\theta$ ,  $\phi$ ). The initial Gaussian wave packet has a width  $\delta = 0.45$  and initial kinetic energy  $E_0 = 0.40$  eV.

by hydrogen from the N-terminal shown in Figure 1 will result in significant T–T energy transfer.

3. Large angular excitation of torsion occurs at collision angles where strong energy transfer is observed, and the two are closely correlated.

**Acknowledgment.** This work is supported in part by the National Science Foundation Grant CHE0072183 and Petroleum Research Fund administered by the American Chemical Society.

## References and Notes

- (1) Hill, J. R.; Dlott, D. D.; Rella, C. W.; et al. *Biospectroscopy* **1996**, 2, 277.
- (2) Clary, D. C.; Meijer, A. J. H. M. *J. Chem. Phys.* **2002**, 116, 9829.
- (3) Miller, W. H.; Hase, W. L.; Darling, C. L. *J. Chem. Phys.* **1989**, 91, 2863.
- (4) Ben-Nun, M.; Levine, R. D. *J. Chem. Phys.* **1996**, 105, 8136.
- (5) Branden, C.; Tooze, J. *Introduction to Protein Structure*; Garland Publishing: New York and London, 1991.
- (6) Guntert, P. *Q. Rev. Biophys.* **1968**, 31, 145.
- (7) Zhang, D. W.; Wang, M. L.; Zhang, J. Z. H. *J. Chem. Phys.*, in press.
- (8) Anne-Marie, S. *Molecular Orbital Calculations for Biological Systems*; Oxford University Press: Oxford, U.K., 1998.
- (9) Goldflam, R.; Green, S.; Kouri, D. J. *J. Chem. Phys.* **1977**, 67, 4149.
- (10) Mowrey, R. C.; Kouri, D. J. *J. Chem. Phys.* **1986**, 84, 6466.
- (11) Kosloff, R. *J. Phys. Chem.* **1988**, 92, 2087.
- (12) Zhang, D. H.; Zhang, J. Z. H. in *Dynamics of Molecules and Chemical Reactions*; Wyatt, R. E., Zhang, J. Z. H., Eds.; Marcel Dekker: New York, 1996.
- (13) Zhang, J. Z. H. *Theory and Application of Quantum Molecular Dynamics* World Scientific: Singapore, 1999.
- (14) Fleck, J. A.; Morris, J. R., Jr.; Feit, M. D. *Appl. Phys.* **1976**, 10, 129.
- (15) Frisch, M. J.; Trucks, G. W.; Schlegel, H. B.; Scuseria, G. E.; Robb, M. A.; Cheeseman, J. R.; Zakrzewski, V. G.; Montgomery, J. A., Jr.; Stratmann, R. E.; Burant, J. C.; Dapprich, S.; Millam, J. M.; Daniels, A. D.; Kudin, K. N.; Strain, M. C.; Farkas, O.; Tomasi, J.; Barone, V.; Cossi, M.; Cammi, R.; Mennucci, B.; Pomelli, C.; Adamo, C.; Clifford, S.; Ochterski, J.; Petersson, G. A.; Ayala, P. Y.; Cui, Q.; Morokuma, K.; Malick, D. K.; Rabuck, A. D.; Raghavachari, K.; Foresman, J. B.; Cioslowski, J.; Ortiz, J. V.; Stefanov, B. B.; Liu, G.; Liashenko, A.; Piskorz, P.; Komaromi, I.; Gomperts, R.; Martin, R. L.; Fox, D. J.; Keith, T.; Al-Laham, M. A.; Peng, C. Y.; Nanayakkara, A.; Gonzalez, C.; Challacombe, M.; Gill, P. M. W.; Johnson, B. G.; Chen, W.; Wong, M. W.; Andres, J. L.; Head-Gordon, M.; Replogle, E. S.; Pople, J. A. *Gaussian 98*, revision A.6; Gaussian, Inc.: Pittsburgh, PA, 1998.
- (16) Zhang, D. W.; Li, Y. M.; Zhang, J. Z. H. *J. Theor. Comput. Chem.*, in press.